

DETECTION OF GRAVITATIONAL WAVES FROM INFLATION

MARC KAMIONKOWSKI*

*California Institute of Technology, Mail Code 130-33
Pasadena, CA 91125, USA*

ANDREW H. JAFFE†

*Center for Particle Astrophysics, 301 LeConte Hall, University of California
Berkeley, CA 94720, USA*

Recent measurements of temperature fluctuations in the cosmic microwave background (CMB) indicate that the Universe is flat and that large-scale structure grew via gravitational infall from primordial adiabatic perturbations. Both of these observations seem to indicate that we are on the right track with inflation. But what is the new physics responsible for inflation? This question can be answered with observations of the polarization of the CMB. Inflation predicts robustly the existence of a stochastic background of cosmological gravitational waves with an amplitude proportional to the square of the energy scale of inflation. This gravitational-wave background induces a unique signature in the polarization of the CMB. If inflation took place at an energy scale much smaller than that of grand unification, then the signal will be too small to be detectable. However, if inflation had something to do with grand unification or Planck-scale physics, then the signal is conceivably detectable in the optimistic case by the Planck satellite, or if not, then by a dedicated post-Planck CMB polarization experiment. Realistic developments in detector technology as well as a proper scan strategy could produce such a post-Planck experiment that would improve on Planck's sensitivity to the gravitational-wave background by several orders of magnitude in a decade timescale.

1. What Have We Learned from the Cosmic Microwave Background?

The past year has seen spectacular advances in measurements of temperature fluctuations in the cosmic microwave background (CMB)^{1,2,3} that have led to major advances in our ability to characterize the largest-scale structure of the Universe, the origin of density perturbations, and the early Universe. The primary aim of these experiments has been to determine the power spectrum, C_ℓ , of the CMB as a function of multipole moment ℓ . Given a map of the temperature $T(\hat{\mathbf{n}})$ in each direction $\hat{\mathbf{n}}$ on the sky, the power spectrum can be obtained by expanding in spherical harmonics,

$$a_{\ell m} = \int d\hat{\mathbf{n}} Y_{\ell m}(\hat{\mathbf{n}}) T(\hat{\mathbf{n}}), \quad (1)$$

and then squaring and summing the coefficients,

$$C_\ell = \frac{1}{2\ell + 1} \sum_m |a_{\ell m}|^2. \quad (2)$$

*kamion@tapir.caltech.edu

†jaffe@cfpa.berkeley.edu

If the map covers a patch of the sky that is small enough to be approximated as a flat surface, the power spectrum can be written in terms of Fourier coefficients:

$$T_{\vec{\ell}} = \int d\hat{\mathbf{n}} e^{-i\vec{\ell}\cdot\vec{\theta}} T(\hat{\mathbf{n}}), \quad (3)$$

and then

$$C_\ell \simeq \langle |T_{\vec{\ell}}|^2 \rangle_{|\ell|=\ell}, \quad (4)$$

where the average is taken over all Fourier coefficients $\vec{\ell}$ that have amplitude ℓ . Thus, each multipole moment C_ℓ measures, roughly speaking, the rms temperature fluctuation between two points separated by an angle $\theta \simeq (\ell/200)^{-1}$ degrees on the sky.

Recent experiments have sought to determine the power spectrum in the range $50 \lesssim \ell \lesssim 1000$, as structure-formation theories predict a series of bumps in this regime that arise as consequences of oscillations in the baryon-photon fluid in the era before recombination (as indicated by the curves in Fig. 1). The rich structure in these peaks, which can be characterized, e.g., by the precise heights and widths of the peaks, their locations in ℓ , and the heights of the troughs between the peaks, depends in detail on the values of several classical cosmological parameters, such as the baryon density Ω_b (in units of the critical density), Hubble constant h (in units of 100 km/sec/Mpc), matter density Ω_m , and cosmological constant Ω_Λ ; on structure-formation parameters such as the amplitude and spectral index of primordial perturbations^{5,6}; and on the character of primordial perturbations (e.g., adiabatic, isocurvature, or topological-defects products). In particular, the location of the first peak depends primarily on the geometry of the Universe (parameterized by the *total* density Ω_{tot}), and only secondarily on the other cosmological parameters⁷. If the Universe is flat, the first peak is expected to occur at $\ell \sim 200$, while if the Universe has a matter density $\Omega_m \sim 0.3$ (as dynamical measurements indicate) but is open (no cosmological constant), then the first peak should be at $\ell \sim 500$.

Experiments that measure the power spectrum in the regime $50 \lesssim \ell \lesssim 1000$ require high sensitivity to detect the CMB temperature variations of roughly one part in 100,000, and they require subdegree angular resolution. Within the past year, the first high-signal-to-noise high-angular-resolution maps of the CMB have been published by the BOOMERanG² and MAXIMA³ collaborations. The results of a joint analysis⁴ of the data from both BOOMERANG and MAXIMA are shown in Fig. 1. The data show a peak at $\ell \sim 200$ which provides very strong evidence that the Universe is flat (earlier measurements by the TOCO collaboration¹ also indicated a first peak at $\ell \sim 200$, but with lower signal-to-noise). The peak structure is also very consistent with growth of large-scale structure from a nearly scale-invariant spectrum of primordial adiabatic perturbations and very *inconsistent* with isocurvature or topological-defect alternatives. The peak structure indicated in Fig. 1 is also beginning to provide valuable information about the values of other cosmological parameters^{8,9}.

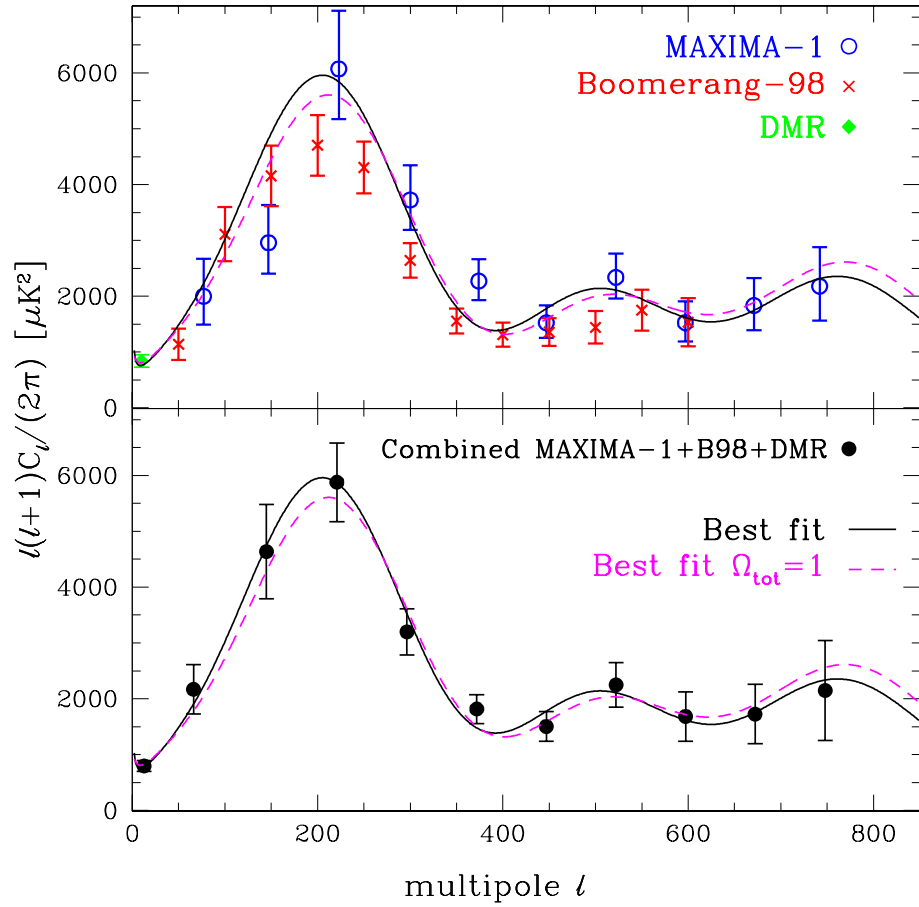


Fig. 1. Data points on the CMB temperature power spectrum obtained individually by BOOMERanG and MAXIMA, as well as the points obtained from a joint analysis of the two data sets. The data indicate unequivocally a peak at $l \sim 200$ and are beginning to show the outline of a second peak at $l \sim 500$. From Jaffe et al.⁴

2. Inflation and Gravitational Waves

The flatness of the Universe and adiabatic perturbations suggest that we are on the right track with inflation^{10,11,12}, a period of accelerated expansion in the very early Universe driven by the vacuum energy associated with some new ultra-high-energy physics. In order to solve the horizon problem for which it was initially proposed, inflation predicts that the Universe is flat. Moreover, shortly after inflation was proposed, it was realized that vacuum fluctuations in the inflaton (the scalar field responsible for inflation) would produce a nearly-scale-invariant spectrum of adiabatic perturbations^{13,14,15,16,17}. With the advent of these CMB tests, inflation has now had several opportunities to fail empirically, but it has not. Conservatively, these successes are at least suggestive and warrant further tests of inflation.

Perhaps the most promising avenue toward further tests of inflation is the gravitational-wave background. In addition to predicting a flat Universe with adiabatic perturbations, inflation also predicts that quantum fluctuations in the spacetime metric during inflation would give rise to a stochastic gravitational-wave background with a nearly-scale-invariant spectrum¹⁸. Quantum fluctuations in the spacetime metric can only be affected by gravitational effects which are quantified completely during inflation by the expansion rate H_{infl} . This is related through the Friedmann equation to the vacuum-energy density V during inflation, $H_{\text{infl}}^2 = 8\pi V/(3m_{\text{Pl}}^2)$, where m_{Pl} is the Planck mass ($m_{\text{Pl}}^{-2} = G$, Newton’s constant, in particle-physics units $\hbar = c = 1$). Thus, the amplitude of the gravitational-wave background is fixed entirely by the vacuum-energy density during inflation, which itself should be proportional to the fourth power of the energy scale E_{infl} of the new physics responsible for inflation. The spectrum of gravitational waves depends on the particular inflationary model, but in most models (and certainly in the simplest inflationary models), it is likely to be very close to scale invariant.

These gravitational waves will produce temperature fluctuations at large angles ($\ell \lesssim 1100$) in the CMB (as shown in Fig. 2). The amplitude of their contribution to the CMB temperature quadrupole can be written¹⁹

$$\mathcal{T} \equiv 6 C_2^{\text{TT,tensor}} = 9.2 \frac{V}{m_{\text{Pl}}^4}, \quad (5)$$

(where “tensor” refers to gravitational waves, as they are tensor perturbations to the spacetime metric and “TT” refers to the temperature quadrupole). Since the quadrupole measured by *COBE*, $C_2^{\text{TT}} = (1.0 \pm 0.1) \times 10^{-10}$, is most generally due to some combination of density perturbations and gravitational waves, we already have an important constraint to the energy scale of inflation: $V^{1/4} \lesssim 2 \times 10^{16}$ GeV.^{19,20}

3. Gravitational Waves and Polarization

But how can we go further? One might think that improved temperature maps could be used to measure the power spectrum well enough to distinguish the relative contributions of the gravitational-wave and density-perturbation power spectra

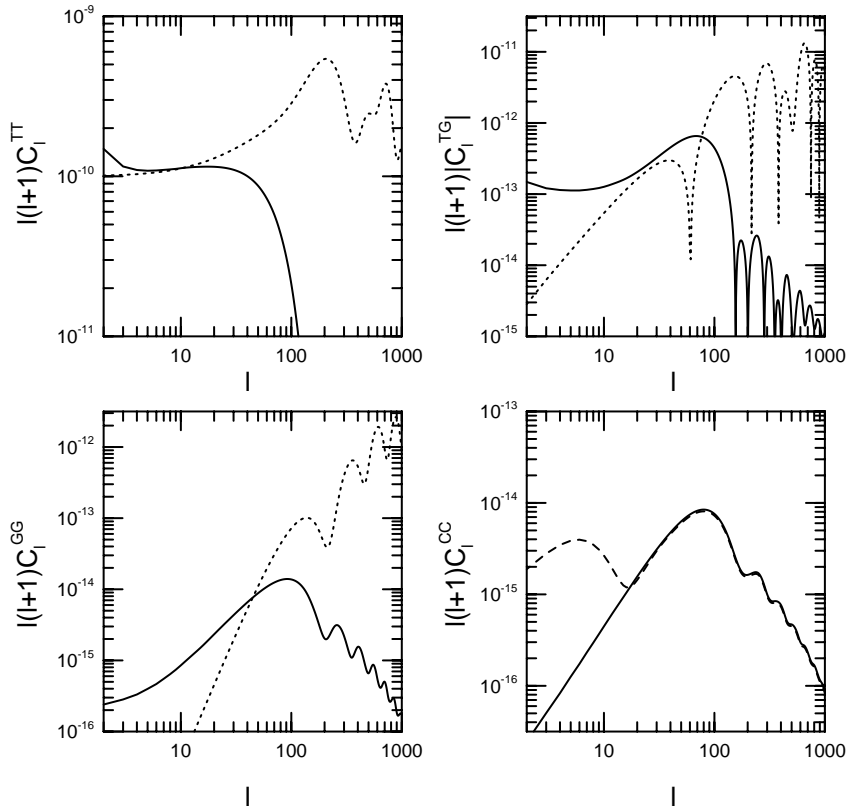


Fig. 2. Temperature and polarization power spectra from density perturbations (dotted curves) and gravitational waves (solid curves). The absence of a dotted curve for the CC (lower right-hand) panel is due to the fact that density perturbations do not produce a curl component. The solid curves show predictions for a model in which there is no reionization. More realistically some fraction $\tau \sim 0.1$ of the CMB photons will have re-scattered from reionized gas, and this will generate additional polarization power at large angles, as indicated by the dashed curve in the CC panel.

indicated in the upper left panel of Fig. 2. However, the precision with which the power spectrum can be measured is limited even in an ideal experiment by cosmic variance, the sample variance due to the fact that we have only $2\ell + 1$ independent modes with which to measure each C_ℓ .

Instead, progress can be made with the polarization of the CMB. In addition to producing temperature fluctuations, both gravitational waves and density perturbations will produce linear polarization in the CMB, and the polarization patterns produced by each differ. This can be quantified with a harmonic decomposition of the polarization field. The linear-polarization state of the CMB in a direction $\hat{\mathbf{n}}$ can be described by a symmetric trace-free 2×2 tensor,

$$\mathcal{P}_{ab}(\hat{\mathbf{n}}) = \frac{1}{2} \begin{pmatrix} Q(\hat{\mathbf{n}}) & -U(\hat{\mathbf{n}}) \sin \theta \\ -U(\hat{\mathbf{n}}) \sin \theta & -Q(\hat{\mathbf{n}}) \sin^2 \theta \end{pmatrix}, \quad (6)$$

where the subscripts ab are tensor indices, and $Q(\hat{\mathbf{n}})$ and $U(\hat{\mathbf{n}})$ are the Stokes parameters. Just as the temperature map can be expanded in terms of spherical harmonics, the polarization tensor can be expanded,^{21,22,23,24}

$$\frac{\mathcal{P}_{ab}(\hat{\mathbf{n}})}{T_0} = \sum_{lm} \left[a_{(lm)}^G Y_{(lm)ab}^G(\hat{\mathbf{n}}) + a_{(lm)}^C Y_{(lm)ab}^C(\hat{\mathbf{n}}) \right], \quad (7)$$

in terms of tensor spherical harmonics, $Y_{(lm)ab}^G$ and $Y_{(lm)ab}^C$. It is well known that a vector field can be decomposed into a curl and a curl-free (gradient) part. Similarly, a 2×2 symmetric traceless tensor field can be decomposed into a tensor analogue of a curl and a gradient part; the $Y_{(lm)ab}^G$ and $Y_{(lm)ab}^C$ form a complete orthonormal basis for the “gradient” (i.e., curl-free) and “curl” components of the tensor field, respectively.[‡] Lengthy but digestible expressions for the $Y_{(lm)ab}^G$ and $Y_{(lm)ab}^C$ are given in terms of derivatives of spherical harmonics and also in terms of Legendre functions in Kamionkowski et al.²² The mode amplitudes in Eq. (7) are given by

$$\begin{aligned} a_{(lm)}^G &= \frac{1}{T_0} \int d\hat{\mathbf{n}} \mathcal{P}_{ab}(\hat{\mathbf{n}}) Y_{(lm)ab}^{G*}(\hat{\mathbf{n}}), \\ a_{(lm)}^C &= \frac{1}{T_0} \int d\hat{\mathbf{n}} \mathcal{P}_{ab}(\hat{\mathbf{n}}) Y_{(lm)ab}^{C*}(\hat{\mathbf{n}}), \end{aligned} \quad (8)$$

which can be derived from the orthonormality properties of these tensor harmonics²². Thus, given a polarization map $\mathcal{P}_{ab}(\hat{\mathbf{n}})$, the G and C components can be isolated by first carrying out the transformations in Eq. (8) to the $a_{(lm)}^G$ and $a_{(lm)}^C$, and then summing over the first term on the right-hand side of Eq. (7) to get the G component and over the second term to get the C component. (In practice, a full likelihood formalism would be used to determine the spectra in the presence of anisotropic, correlated noise, astrophysical foregrounds, and incomplete sky coverage.)

The two-point statistics of the combined temperature/polarization (T/P) map are specified completely by the six power spectra $C_\ell^{XX'}$ for $X, X' = \{T, G, C\}$. Parity

[‡]Our G and C are sometimes referred to as the “scalar” and “pseudo-scalar” components²⁵, respectively, or with slightly different normalization as E and B modes²⁴ (although these should not be confused with the radiation’s electric- and magnetic-field vectors).

invariance demands that $C_\ell^{\text{TC}} = C_\ell^{\text{GC}} = 0$ (unless the physics that gives rise to CMB fluctuations is parity breaking^{26,27}). Therefore, the statistics of the CMB temperature-polarization map are completely specified by the four sets of moments: C_ℓ^{TT} , C_ℓ^{TG} , C_ℓ^{GG} , and C_ℓ^{CC} .

Both density perturbations and gravitational waves will produce a gradient component in the polarization. However, only gravitational waves will produce a curl component^{21,23} (but see below). The curl component thus provides a model-independent probe of the gravitational-wave background, and it is thus the CMB polarization component that we focus on here.

4. Detectability of the Curl Component

If our goal is to detect the polarization signature of gravitational waves, what is the optimum experiment? What is the ideal angular resolution and survey size? What instrumental sensitivity is required? This article will address these questions (although fall a bit short of providing a complete answer).

If we are interested only in the gravitational-wave signature, we can focus on the model-independent curl component of the polarization produced by gravitational waves. In this article, we summarize work reported in Jaffe et al.,²⁸ a paper that extends the work of Kamionkowski and Kosowsky²⁹ and Lesgourgues et al.³⁰ § We ask, what is the smallest amplitude of a curl component from an inflationary gravitational-wave background that could be distinguished from the null hypothesis of no curl component by an experiment that maps the polarization over some fraction of the sky with a given angular resolution and instrumental noise? If an experiment concentrates on a smaller region of sky, then several things happen that affect the sensitivity: (1) information from modes with $\ell \lesssim 180/\theta$ (where θ^2 is the area on the sky mapped) is lost; ¶(2) the sample variance is increased; (3) the noise per pixel is decreased since more time can be spent integrating on this smaller patch of the sky.

More concretely, suppose we hypothesize that there is a C component of the polarization with a power spectrum that has the ℓ dependence expected from inflation, as shown in Fig. 2, but an unknown amplitude \mathcal{T} . We can predict the size of the error that we will obtain from the ensemble average of the curvature of the likelihood function (also known as the Fisher matrix)^{5,6}. In such a likelihood analysis, the expected error on the gravitational-wave amplitude \mathcal{T} will be $\sigma_{\mathcal{T}}$, where

$$\frac{1}{\sigma_{\mathcal{T}}^2} = \sum_{\ell} \left(\frac{\partial C_{\ell}^{\text{CC}}}{\partial \mathcal{T}} \right)^2 \frac{1}{(\sigma_{\ell}^{\text{CC}})^2}. \quad (9)$$

§There is also related work in Kinney³², Zaldarriaga et al.³³, and Copeland et al.³⁴ in which it is determined how accurately various cosmological and inflationary parameters can be determined in case of a positive detection. Magueijo and Hobson^{35,36} presented arguments regarding partial-sky coverage for temperature maps analogous to those for polarization maps presented here.

¶This is not strictly true. In principle, as usual in Fourier analysis, less sky coverage merely limits the independent modes one can measure to have a spacing of $\delta\ell \gtrsim 180/\theta$. In practice, instrumental effects (detector drifts; “1/f” noise) will render the smallest of these bins unobservable.

Here, the σ_ℓ^{CC} are the expected errors at individual ℓ for each C_ℓ^{CC} multipole moments. These are given by (cf., Kamionkowski et al.²²)

$$\sigma_\ell^{\text{CC}} = \sqrt{\frac{2}{f_{\text{sky}}(2\ell+1)}} (C_\ell^{\text{CC}} + f_{\text{sky}}w^{-1}B_\ell^{-2}), \quad (10)$$

where $w^{-1} = 4\pi s^2/(t_{\text{pix}}N_{\text{pix}}T_0^2)$ is the variance (inverse weight) per unit area on the sky, f_{sky} is the fraction of the sky observed, and t_{pix} is the time spent observing each of the N_{pix} pixels. The detector sensitivity is s and the average sky temperature is $T_0 = 2.73 \mu\text{K}$ (and hence the C_ℓ^{CC} are measured in units that have been scaled by T_0). The inverse weight for a full-sky observation is $w^{-1} = 2.14 \times 10^{-15} t_{\text{yr}}^{-1} (s/200 \mu\text{K} \sqrt{\text{sec}})^2$ with t_{yr} the total observing time in years. Finally, B_ℓ is the experimental beam, which for a Gaussian is $B_\ell = e^{-\ell^2 \sigma_b^2/2}$. We assume all detectors are polarized.

The error to C_ℓ^{CC} has two terms, one proportional to C_ℓ^{CC} (the *sample variance*), and another proportional to w^{-1} (the *noise variance*). There are several complications to note when considering these formulae: 1) We never have access to the actual C_ℓ^{CC} , but only to some estimate of the spectra; 2) the expressions only deal approximately with the effect of partial sky coverage; and 3) the actual likelihood function can be considerably non-Gaussian, so the expressions above do not really refer to “1 σ confidence limits.”

Here, we are interested in the detectability of the curl component; that is, what is the smallest gravitational-wave amplitude that we could confidently differentiate from zero? Toy problems and experience give us an approximate rule of thumb: the signal is detectable when it can be differentiated from the “null hypothesis” of $C_\ell^{\text{CC}} = 0$. Thus, the ℓ component of the gravitational-wave signal is detectable if its amplitude is greater than

$$\sigma_\ell^{\text{CC}} = \sqrt{2/(2\ell+1)} f_{\text{sky}}^{1/2} w^{-1} e^{\ell^2 \sigma_b^2}. \quad (11)$$

We then estimate the smallest gravitational-wave amplitude \mathcal{T} that can be distinguished from zero (at “1 sigma”) by using Eq. (9) with the null hypothesis $C_\ell^{\text{CC}} = 0$. Putting it all together, the smallest detectable gravitational-wave amplitude (scaled by the largest consistent with *COBE*) is

$$\frac{\sigma_{\mathcal{T}}}{\mathcal{T}} \simeq 1.47 \times 10^{-17} t_{\text{yr}} \left(\frac{s}{200 \mu\text{K} \sqrt{\text{sec}}} \right)^2 \left(\frac{\theta}{\text{deg}} \right) \Sigma_\theta^{-1/2}, \quad (12)$$

where

$$\Sigma_\theta = \sum_{\ell \geq (180/\theta)} (2\ell+1) (C_\ell^{\text{CC}})^2 e^{-2\ell^2 \sigma_b^2}. \quad (13)$$

Results of the calculation are shown in Fig. 3. Plotted there is the smallest gravitational-wave amplitude \mathcal{T} detectable at 3σ by an experiment with a detector sensitivity $s = 10 \mu\text{K} \sqrt{\text{sec}}$ that maps a square region of the sky over a year with a given beamwidth. The horizontal line shows the upper limit to the

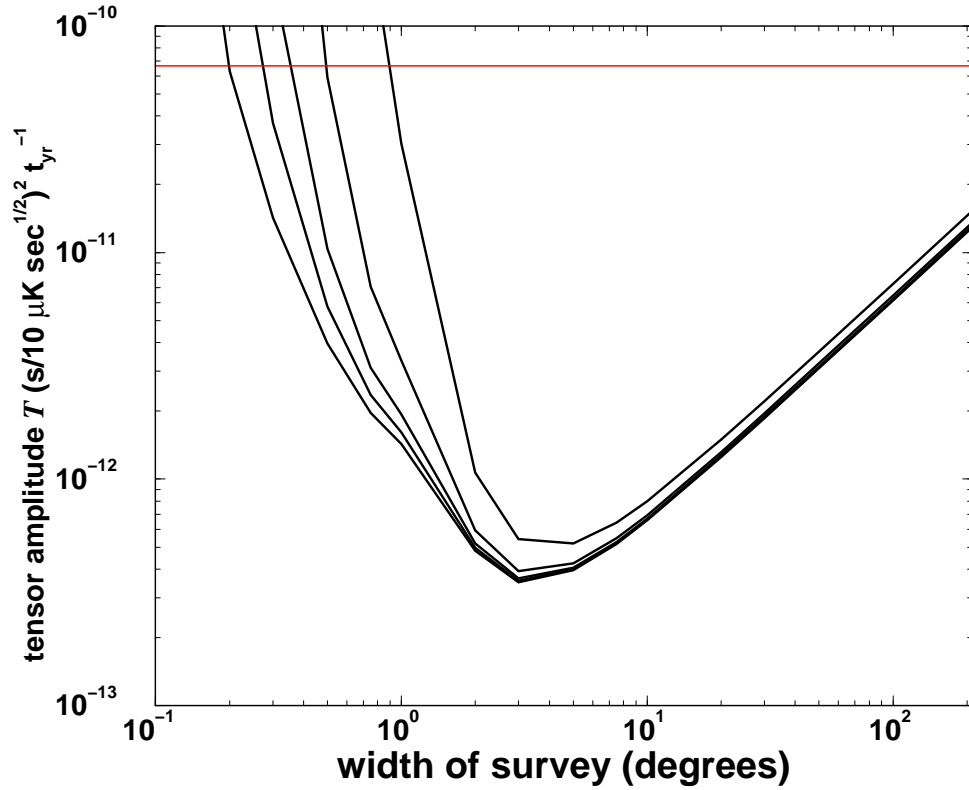


Fig. 3. The smallest gravitational-wave (tensor) amplitude \mathcal{T} that could be detected at 3σ with an experiment with a detector sensitivity $s = 10 \mu\text{K}\sqrt{\text{sec}}$ that runs for one year and maps a square region of the sky of a given width. The result scales with the square of the detector sensitivity and inversely with the duration of the experiment. The curves are (from top to bottom) for fwhm beamwidths of 1, 0.5, 0.3, 0.2, and 0.1 degrees. The horizontal line shows the upper limit to the gravitational-wave amplitude from *COBE*.

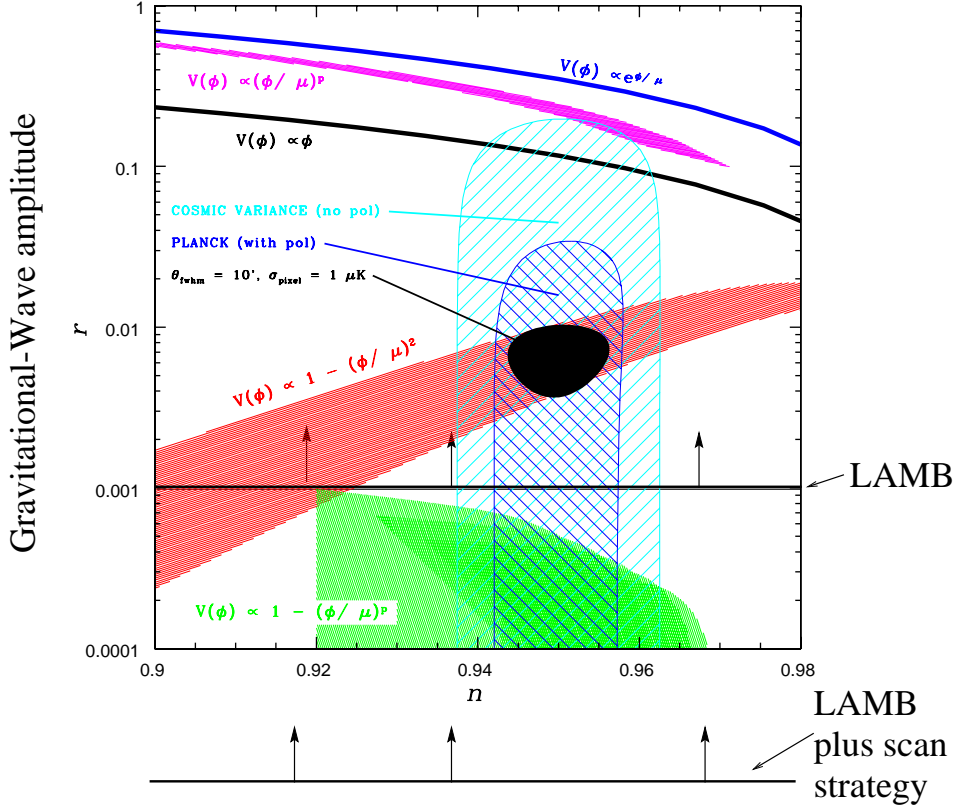


Fig. 4. Regions in the r - n parameter space occupied by various inflationary models, as well as those regions that could be detected by various CMB experiments. Here r measures the gravitational-wave amplitude (or alternatively, the energy scale of inflation) and n the spectral index for primordial perturbations. Adapted from Kinney³². See text for more details.

gravitational-wave amplitude from *COBE*. The curves are (from top to bottom) for fwhm beamwidths of 1, 0.5, 0.3, 0.2, 0.1, and 0.05 degrees. The results scale with the square of the detector sensitivity and inversely to the duration of the experiment.

The sensitivity to the gravitational-wave signal is a little better with an 0.5-degree beam than with a 1-degree beam, but even better angular resolution does not improve the sensitivity much. And with a resolution of 0.5 degrees or better, the best survey size for detecting this gravitational-wave signal is about 3 to 5 degrees. If such a fraction of the sky is surveyed, the sensitivity to a gravitational-wave signal (rms) will be about 30 times better than with a full-sky survey with the same detector sensitivity and duration (and thus 30 times better than indicated in Kamionkowski and Kosowsky^{29,19}). Thus, a balloon experiment with the same detector sensitivity as MAP could in principle detect the same gravitational-wave amplitude in a few weeks that MAP would in a year. (A width of 200 degrees corresponds to full-sky coverage.)

Since the gravitational-wave amplitude is related to the energy scale of inflation, Fig. 3 determines the inflationary energy scale accessible with any given experiment. Some indication of the range of inflationary models that can be probed with past, current, and future experiments is provided in Fig. 4, adapted from Kinney³². The parameter r (y axis) increases with increasing gravitational-wave amplitude, or alternatively, with the energy scale of inflation. The shaded regions show the where the predictions for various classes of inflationary models (e.g., exponential, power-law, etc; for more details see Kinney et al.^{31,32}). The scored region labeled “COSMIC VARIANCE (no pol)” shows the region of parameter space that would be consistent with a null search for gravitational waves *without* polarization, while that labeled “PLANCK (with pol)” shows regions of parameter space that would be consistent with a null search for the curl component in the Planck satellite³⁷, an ESA CMB mission scheduled for launch in 2007 (in both cases, it is assumed that $n = 0.95$).

How much could the sensitivity be improved with a post-Planck dedicated polarization experiment? Achieving the Planck sensitivity will be no small feat for experiment, and improvements will require considerable ingenuity. Still, there are prospects for improvements. Very conservatively, a factor-of-3 improvement over Planck’s detector sensitivity is plausible. The dark ellipse labeled “ $\theta_{\text{fwhm}} = 10^\circ$, $\sigma_{\text{pixel}} = 1\mu\text{K}$ ” is the error ellipse that could be obtained by a putative experiment with roughly a factor-of-3 improvement to Planck’s detector sensitivity, assuming that the true gravitational-wave amplitude and spectral index lie at the center of that ellipse.

There are good reasons to believe that technological developments in the next few years may allow further improvements in detector sensitivity, perhaps of an order of magnitude over that achieved in Planck. As an example, we mention LAMB (Large-Format Array of Microwave Bolometers)³⁸, a new detector concept that would allow roughly an order-of-magnitude improvement over Planck’s detector sensitivity with a much smaller instrument. If we assume that such a detector can be developed and flown in an all-sky survey, the factor-of-ten improvement would allow us to access the regions of parameter space that lie above the line labeled “LAMB” in Fig. 4. If this experiment additionally spent its time surveying a smaller region of the sky, then the regions of inflationary parameter space that could be accessed would be those that lie above the line labeled “LAMB plus scan strategy.”

5. Conclusions

We have carried out calculations that will help assess the prospects for detection of the curl component of the polarization with various experiments. Our results can be used to forecast the signal-to-noise for the gravitational-wave signal in an experiment of given sky coverage, angular resolution, and instrumental noise. Of course, the “theoretical” factors considered here must be weighed in tandem with those that involve foreground subtraction and experimental logistics in the design or evaluation of any particular experiment. These usually encourage increasing the

signal-to-noise and sky coverage to better isolate experimental systematics.

In contrast to temperature anisotropies which show power on all scales [i.e., $\ell(\ell + 1)C_\ell \sim \text{const}$], the polarization power peaks strongly at higher ℓ . Hence the signal-to-noise in a polarization experiment of fixed flight time and instrumental sensitivity may be improved by surveying a smaller region of sky, unlike the case for temperature-anisotropy experiments. The ideal survey for detecting the curl component from gravitational waves is of order 2–5 degrees, and the sensitivity is not improved much for angular resolutions smaller than 0.2 degrees. An experiment with this ideal sky coverage could improve on the sensitivity to gravitational waves of a full-sky experiment by roughly a factor of 30. When coupled with realistic forecasts for improvements in detector sensitivity, we find that an experiment that accesses a very good fraction of the inflationary parameter space (specifically, most of the inflationary parameter space associated with grand unification) is conceivable in the not-too-distant future.

Before closing, we should note that secondary (in the density-perturbation amplitude) effects such as weak gravitational lensing³⁹ or re-scattering of CMB photons from reionized gas⁴⁰ may lead to the production of a curl component in the CMB, even in the absence of gravitational waves. However, these secondary effects should be distinguishable from those of gravitational waves, as they produce a curl component primarily at angular scales much smaller than those at which the gravitational-wave signal should show up. Of course, an angular resolution better than that we have suggested here and a survey area a bit larger than we have suggested here may be required to distinguish the gravitational-wave signal from these other sources of a curl component (as well as from foregrounds). A more complete assessment of the impact of these secondary effects on the detectability of gravitational waves is now underway⁴¹.

Finally, the CMB polarization will be useful for a wide variety of other purposes in cosmology. For example, detection, and ultimately mapping, of the polarization will help isolate the peculiar velocity at the surface of last scatter⁴², constrain the ionization history of the Universe⁴³, determine the nature of primordial perturbations^{44,45}, probe primordial magnetic fields^{46,47,48} and cosmological parity violation^{26,27}, and maybe more (see, e.g., Kamionkowski and Kosowsky¹⁹ for a recent review).

Acknowledgments

MK was supported in part by NSF AST-0096023, NASA NAG5-8506, and DoE DE-FG03-92-ER40701. AHJ was supported by NSF KDI grant 9872979 and NASA LTSA grant NAG5-6552.

1. A. D. Miller et al., *Astrophys.J.* **524**, L1 (1999).
2. P. de Bernardis et al., *Nature* **404**, 955 (2000).
3. S. Hanany et al., *Astrophys. J. Lett.*, in press [astro-ph/0005123].
4. A. H. Jaffe et al., astro-ph/0007333.

5. G. Jungman, M. Kamionkowski, A. Kosowsky and D. N. Spergel, *Phys. Rev. Lett.* **76**, 1007 (1996)
6. G. Jungman, M. Kamionkowski, A. Kosowsky and D. N. Spergel, *Phys. Rev. D* **54**, 1332 (1996).
7. M. Kamionkowski, D. N. Spergel and N. Sugiyama, *Astrophys. J. Lett.* **426**, L57 (1994).
8. A. E. Lange et al., astro-ph/0005004
9. M. Balbi et al., astro-ph/0005124.
10. A. H. Guth, *Phys. Rev. D* **28**, 347 (1981).
11. A. D. Linde, *Phys. Lett. B* **108**, 389 (1982).
12. A. Albrecht and P. J. Steinhardt, *Phys. Rev. Lett.* **48**, 1220 (1982).
13. A. H. Guth and S.-Y. Pi, *Phys. Rev. Lett.* **49**, 1110 (1982).
14. S. W. Hawking, *Phys. Lett. B* **115**, 29 (1982).
15. A. D. Linde, *Phys. Lett. B* **116**, 335 (1982).
16. A. A. Starobinsky, *Phys. Lett. B* **117**, 175 (1982).
17. J. M. Bardeen, P. J. Steinhardt and M. S. Turner, *Phys. Rev. D* **46**, 645 (1983).
18. L. F. Abbott and M. Wise, *Nucl. Phys. B* **244**, 541 (1984).
19. M. Kamionkowski and A. Kosowsky, *Ann. Rev. Nucl. Part. Sci.* **49**, 77 (1999).
20. J. P. Zibin, D. Scott D and M. White, *Phys. Rev. D* **60**, 123513 (1999).
21. M. Kamionkowski, A. Kosowsky and A. Stebbins, *Phys. Rev. Lett.* **78**, 2058 (1997).
22. M. Kamionkowski, A. Kosowsky and A. Stebbins, *Phys. Rev. D* **55**, 7368 (1997).
23. U. Seljak and M. Zaldarriaga, *Phys. Rev. Lett.* **78**, 2054 (1997).
24. M. Zaldarriaga and U. Seljak, *Phys. Rev. D* **55**, 1830 (1997).
25. A. Stebbins, astro-ph/9609149.
26. A. Lue, L. Wang and M. Kamionkowski, *Phys. Rev. Lett.* **83**, 1503 (1999).
27. N. Lepora, gr-qc/9812077.
28. A. H. Jaffe, M. Kamionkowski and L. Wang, *Phys. Rev. D* **61**, 083501 (2000).
29. M. Kamionkowski and A. Kosowsky, *Phys. Rev. D* **57**, 685 (1998).
30. J. Lesgourgues et al., *Astron. Astrophys.* **359**, 414 (2000).
31. W. Kinney, S. Dodelson and E. W. Kolb, *Phys. Rev. D* **56**, 3207 (1998).
32. W. H. Kinney, *Phys. Rev. D* **58**, 123506 (1998).
33. M. Zaldarriaga, U. Seljak and D. N. Spergel, *Astrophys. J.* **488**, 1 (1997).
34. E. J. Copeland, I. J. Grivell and A. R. Liddle, *Mon. Not. R. Astron. Soc.* **298**, 1233 (1998).
35. J. Magueijo and M. P. Hobson, *Phys. Rev. D* **56**, 1908 (1997).
36. M. P. Hobson and J. Magueijo, *Mon. Not. R. Astron. Soc.* **283**, 1133 (1996).
37. <http://astro.estec.esa.nl/SA-general/Projects/Planck/>
38. J. J. Bock, W. Jones, A. E. Lange and J. Zmuidzinas, private communication.
39. M. Zaldarriaga and U. Seljak, *Phys. Rev. D* **58**, 023003 (1998).
40. W. Hu, *Astrophys. J.* **529**, 12 (2000).
41. M. Kesden and M. Kamionkowski, in preparation.
42. M. Zaldarriaga and D. D. Harari, *Phys. Rev. D* **52**, 3276 (1995).
43. M. Zaldarriaga, *Phys. Rev. D* **55**, 1822 (1997).
44. A. Kosowsky, astro-ph/9811163.
45. M. Zaldarriaga and D. N. Spergel, *Phys. Rev. Lett.* **79**, 2180 (1997).
46. A. Kosowsky and A. Loeb, *Astrophys. J.* **469**, 1 (1996).
47. D. D. Harari, J. Hayward and M. Zaldarriaga, *Phys. Rev. D* **55**, 1841 (1996).
48. E. S. Scannapieco and P. G. Ferreira, *Phys. Rev. D* **56**, 4578 (1997).